

Ion-Complex Formation in Aqueous Solutions of Calcium Nitrate. Acoustical Absorption Spectrometry Study

R. Behrends, P. Miecznik,[†] and U. Kaatze*

Drittes Physikalisches Institut, Georg-August-Universität, Bürgerstrasse 42-44, 37073, Göttingen, Germany

Received: November 30, 2001; In Final Form: April 18, 2002

Ultrasonic absorption spectra between 800 kHz and 2 GHz and sound velocities of aqueous solutions of calcium nitrate have been measured at different salt concentrations and temperatures, as well as solutions of calcium chloride and magnesium nitrate at 25 °C. All solutions reveal a relaxation region with discrete relaxation time between 200 and 500 ps (nitrates, 25°) or at 100 ps (chloride, 25°). The amplitude of the relaxation term is substantially larger with the calcium nitrate system than with the other electrolyte solutions with identical salt concentration c . The relaxation time of $\text{Ca}(\text{NO}_3)_2$ solutions is independent of concentration and the relaxation amplitude increases linearly with c , indicating a unimolecular reaction. The high-frequency ultrasonic relaxation is thus assumed to be due to the equilibrium between an outersphere ion complex and a contact ion pair.

Introduction

Electrolyte solutions play a dominant role in many natural and technical systems. Aqueous electrolyte systems are omnipresent in the biosphere. Immense efforts have, therefore, been undertaken in the past to elucidate the properties of ionic solutions.¹ It has been realized for long that the electrostatic forces between the ions are of paramount importance in determining the solution behavior, and it has become increasingly obvious that these forces may result in short-lived ion complexes. Sufficiently sophisticated experimental methods, however, were available only 50 years ago, enabling the kinetics of ion complex formation to be investigated systematically. Particularly matched to the study of fast chemical reactions are methods of acoustical absorption spectrometry and their time-domain analogues, temperature jump, pressure jump, and also field jump techniques.^{2–4} These methods have been extensively used in the past to investigate the kinetics of ion complex formation, including fast proton-transfer reactions.^{2,4–8} Many efforts have been directed toward aqueous solutions of 2:2 and 3:2 valent salts for which the Eigen–Tamm mechanism of stepwise association/dissociation is generally accepted now.^{9–13} Studies of 2:1 valent electrolytes mostly aim at transition metal halides which, due to the specific electronic structure of the cations, form rather exotic complexes.⁴ Prominent examples are zinc chloride solutions. Depending upon the salt concentration mono-, di-, tri-, and tetrachloro complexes may exist in those unusual electrolyte systems,¹⁴ thus attracting much attention by solution chemists. Many biologically relevant molecules, such as carbohydrates and peptides, are complexing agents for divalent alkaline earth metal ions.^{15–17} The coordination of phosphate moieties by cations such as Ca^{2+} is essential for catalytic enzymatic reactions.^{18,19} Despite the important role of calcium ions in biology and medicine, however, little attention has been paid to its characteristics of complex formation with univalent anions.²⁰ Because of the complex physicochemical aspects of the ion complex formation in aqueous solutions of

di-univalent salts and due to the far-reaching biochemical implications of calcium ion complexation, we found it interesting to perform an acoustical absorption spectrometry study of solutions of calcium nitrate in water. The nitrate has been selected from the available calcium salts since solutions of $\text{Ca}(\text{NO}_3)_2$ have been suggested for long to be subject to ion-pair-formation.²¹ For comparison with the behavior of a simpler structured anion, a solution of calcium chloride has also been investigated. A large difference in the catalytic activities of the chemically similar calcium and magnesium ions has been reported,²² pointing at a different effect of the cation radius and/or hydration properties. Therefore, an acoustical spectrum of a $\text{Mg}(\text{NO}_3)_2$ solution has been measured additionally.

Experimental Section

Salt Solutions. $\text{Ca}(\text{NO}_3)_2$ (Fluka, puriss. p.a., >99%), CaCl_2 (Fluka, puriss. p.a., >99%), and $\text{Mg}(\text{NO}_3)_2$ (Merck, p.a., >99%) were used as supplied by the manufacturers. Solutions were prepared by weighing appropriate amounts of the salt into volumetric flasks and by adding double-distilled and deionized water up to the fiduciary mark. The density ρ of the samples has been measured using a pycnometer (20 mL) that had been calibrated against distilled, additionally deionized and degassed water.

Acoustical Absorption Spectrometry. Between 800 kHz and 2 GHz the acoustical absorption coefficient α of the solutions has been determined as a function of frequency ν by spot frequency measurements. Two methods and five different specimen cells have been used to cover the frequency range. At $\nu < 15$ MHz a biplanar cavity resonator method was employed²³ that enables α to be determined relative to a suitably chosen reference liquid. At $\nu > 15$ MHz absolute measurements of α were performed applying a pulse-modulated ultrasonic wave transmission method at variable sample thickness.^{24–26} Four cells were utilized, each specially matched to a particular frequency range (Figure 1). The cells differ from another mainly by their dimensions and by the type of piezoelectric transducers used as transmitter and receiver.

Sound Velocity Measurements. The sound velocity c_s of the samples is obtained as byproduct of the attenuation

* Corresponding author. E-mail: uka@physik3.gwdg.de.

[†] Permanent address: Faculty of Acoustics, Adam Mickiewicz University, Umultowska 85, 61-614 Poznań, Poland.

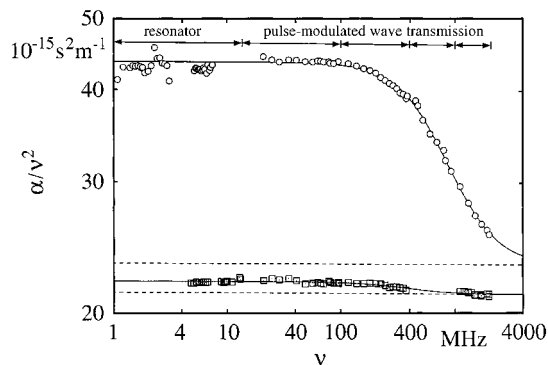


Figure 1. Ultrasonic absorption coefficient α per ν^2 as a function of frequency ν for 1 molar aqueous solutions of $\text{Ca}(\text{NO}_3)_2$ (O) and $\text{Mg}(\text{NO}_3)_2$ (□) at 25 °C. Arrows indicate the frequency ranges of different specimen cells.

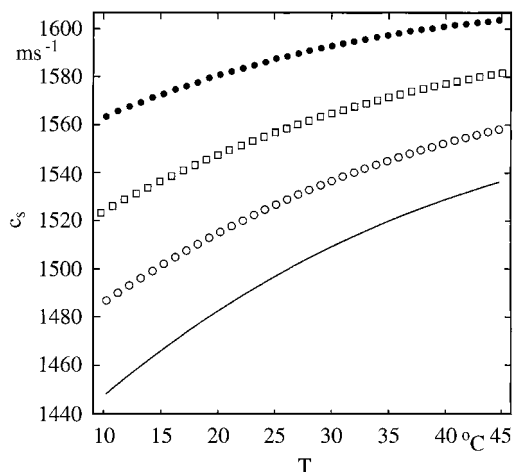


Figure 2. Sound velocity c_s as a function of temperature T for water (full line) and three $\text{Ca}(\text{NO}_3)_2$ solutions (O, 0.5 mol L^{-1} ; □, 1 mol L^{-1} ; ●, 1.5 mol L^{-1}).

coefficient measurements. At low frequencies ($\nu < 15$ MHz), c_s follows from the frequencies of successive principal resonance peaks of the resonator cell. At higher frequencies c_s values can be derived from the waviness of the transfer function of the cell at varying sample thickness, resulting from multiple reflections of the acoustical signal at small transducer spacing. Additionally, we measured the c_s data of three $\text{Ca}(\text{NO}_3)_2$ solutions precisely as a function of temperature T between 10 and 45 °C using a special twin resonator cell method.²⁷ Applying this method, the sound velocity of the sample has been accurately determined relative to c_s of water²⁸ at the same temperature. As shown by Figure 2, the sound velocity of the calcium nitrate solutions do not display anomalies as a function of T .

Experimental Errors. The temperature of the specimen cells was controlled to within ± 0.03 and it was measured with an accuracy of ± 0.02 K. Temperature gradients and differences in the temperature of different cells did not exceed 0.05 K, corresponding to the small estimated error $\Delta\alpha/\alpha < 0.001$ in the absorption coefficient data of the liquids. During the measurements, fluctuations in the frequency of the sonic signal were smaller than $\Delta\nu/\nu = 0.0001$. With the resonator measurements, the main sources of possible errors are small disturbances in the cell geometry and cell adjustment that may have resulted from the cleaning and refilling procedure when the sample liquid was exchanged for the reference. The α values obtained from the pulse-modulated ultrasonic wave transmission measurements may be somewhat affected by an imperfect parallelism of the

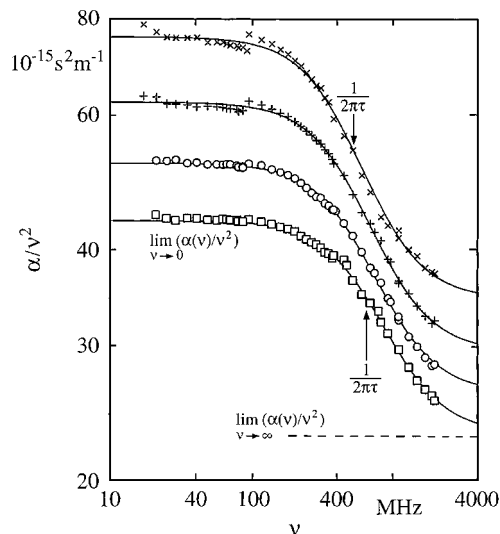


Figure 3. Frequency normalized ultrasonic absorption spectra for the 1 molar aqueous solution of $\text{Ca}(\text{NO}_3)_2$ at four temperatures (\times , 10 °C; +, 15 °C; O, 20 °C; □, 25 °C).

transmitter and receiver transducer unit and, in the lower part of the frequency range of measurement, by insufficient corrections for diffraction losses. The following errors characterize the experimental accuracy of the absorption coefficient data: $\Delta\alpha/\alpha = 0.1$, 0.8–4 MHz; $\Delta\alpha/\alpha = 0.05$, 4–30 MHz; $\Delta\alpha/\alpha = 0.03$, 30–150 MHz; $\Delta\alpha/\alpha = 0.01$, 150–500 MHz; and $\Delta\alpha/\alpha = 0.03$, 500–2000 MHz. The error in the sound velocity data, obtained as a byproduct of the broadband absorption spectrometry, is $\Delta c_s/c_s = 0.005$, 0.8–500 MHz; $\Delta c_s/c_s = 0.01$, 500–2000 MHz. The temperature dependence in the sound velocity at 2 MHz, as measured with the twin cell method, is accurate to within 10^{-5} .

Results and Treatment of Spectra

In Figure 3 frequency normalized acoustical absorption spectra for water + 1 mol/L $\text{Ca}(\text{NO}_3)_2$ are shown at four temperatures. The data display a small but well-defined dispersion ($d(\alpha/\nu^2)/d\nu < 0$) with characteristic frequency $\nu_r = (2\pi\tau)^{-1}$ at some hundred megahertz. Due to thermal activation, this frequency increases with temperature. In correspondence with water the extrapolated high-frequency values $\lim_{\nu \rightarrow \infty} \alpha(\nu)/\nu^2$ decrease with T . Figure 4 shows the spectra of aqueous $\text{Ca}(\text{NO}_3)_2$ solutions at 10 °C for different salt concentrations. To accentuate the high-frequency data the spectra are presented in the format $(\alpha\lambda)_{\text{exc}} - \nu s - \nu$. The excess absorption per wavelength is related to the frequency normalized absorption according to

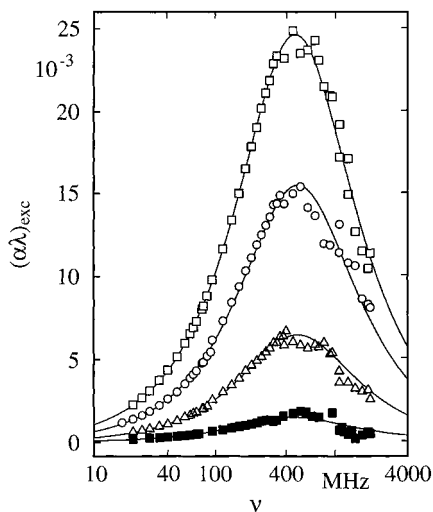
$$(\alpha\lambda)_{\text{exc}} \equiv \alpha\lambda - B\nu = \left[\frac{\alpha}{\nu^2} - \lim_{\nu \rightarrow \infty} \left(\frac{\alpha(\nu)}{\nu^2} \right) \right] c_s \nu \quad (1)$$

with $\lambda = c_s/\nu$ and B independent of ν . Because of the small α values, the corresponding dispersion in the sound velocity of the present solutions is small. Therefore, constant c_s values have been used when transforming the absorption data from one format to the other. The characteristic frequency ν_r , which is the frequency of the maximum of the excess absorption data (Figure 4), obviously is independent of the salt concentration c , whereas the maximum value itself increases monotonically with c .

Similar to the $\text{Mg}(\text{NO}_3)_2$ solution (Figure 1), the spectrum of the CaCl_2 solution exhibits a substantially smaller amplitude

TABLE 1: Molar Concentration c , Sound Velocity c_s , Density ρ , as Well as Relaxation Amplitude A , Relaxation Time τ , and Limiting High-Frequency Absorption-per-Wavelength Parameter B (Eq 2) for the Solutions of 2:1 Valent Salts

solute	c , mol/L $\pm 0.2\%$	T , K $\pm 0.05\%$	c_s , m/s $\pm 0.1\%$	ρ , g/cm ³ $\pm 0.2\%$	A , $10^{-3} \pm 3\%$	τ , ns $\pm 3\%$	B , ps $\pm 1.5\%$
Ca(NO ₃) ₂	0.2	283.15	1465.0	1.030	2.85	0.36	49.4
	0.5	283.15	1486.2	1.0602	12.7	0.32	49.0
	1.0	283.15	1524.1	1.1244	30.9	0.32	52.8
	1.5	283.15	1563.0	1.1752	49.2	0.34	55.4
	1.0	288.15	1536.2	1.1240	28.8	0.28	45.5
	1.0	293.15	1547.0	1.1217	25.0	0.25	40.6
	1.0	298.15	1556.4	1.1152	22.6	0.22	36.6
CaCl ₂	0.5	298.15	1544.7	1.0430	2 \pm 3	0.09 \pm 0.06	33.2
Mg(NO ₃) ₂	1.0	298.15	1577.0	1.0955	0.4 \pm 0.1	0.44 \pm 0.04	33.6


Figure 4. Ultrasonic excess absorption spectra (eq 1) of aqueous solutions of Ca(NO₃)₂ at 10 °C displayed for different concentrations (■, 0.2 mol L⁻¹; △, 0.5 mol L⁻¹; ○, 1 mol L⁻¹; □, 1.5 mol L⁻¹).

than that of the Ca(NO₃)₂ system at the same temperature and concentration.

All measured spectra can be analytically well represented by a relaxation spectral function $R(\nu)$ which is controlled by a discrete relaxation time τ . In terms of absorption-per-wavelength data the spectral function is given by the relation

$$R(\nu) = B\nu + \frac{A\omega\tau}{1 + \omega^2\tau^2} \quad (2)$$

Here, $\omega = 2\pi\nu$ is the angular frequency, $\tau = (2\pi\nu_r)^{-1}$ corresponds with the characteristic (relaxation) frequency ν_r (Figure 3), and the relaxation amplitude is related to the extrapolated high and low frequency α/ν^2 values according to

$$A = \frac{c_s}{2\pi\tau} \left[\lim_{\nu \rightarrow 0} \left(\frac{\alpha(\nu)}{\nu^2} \right) - \lim_{\nu \rightarrow \infty} \left(\frac{\alpha(\nu)}{\nu^2} \right) \right] \quad (3)$$

The relaxation spectral function (eq 2) has been fitted to the measured spectra, using a Marquardt algorithm²⁹ to minimize the variance

$$\chi^2 = \frac{1}{N - P - 1} \sum_{n=1}^N w_n [\alpha(\nu_n)\lambda - R(\nu_n, \varphi_p)]^2 \quad (4)$$

Here N denotes the number of frequency points ν_n per measured spectra and $P(=3)$ is the number of adjustable parameters φ_p ($p = 1, \dots, P$) in $R(\nu_n)$. The w_n ($n = 1, \dots, N$) are weighing factors set inversely proportional to the experimental uncertain-

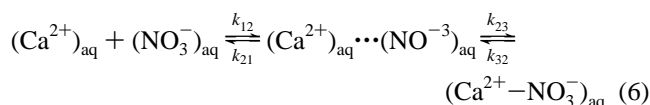
ties $\Delta\alpha(\nu_n)$ of $\alpha(\nu_n)$. The parameter values resulting from the nonlinear least-squares regression analysis of the measured spectra are collected in Table 1.

Discussion

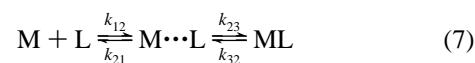
Diffusional Ion Encounter. Constancy, as a function of salt concentration of the relaxation times of Ca(NO₃)₂ solutions, suggests a unimolecular reaction²



Hence, if the sonic absorption spectra are identified with mechanisms of ion complex formation, they must be due to structural isomerization of the complexes rather than the formation of ion structures from cations and anions. Because an ion encounter is a self-evident precondition of complex formation, there must exist at least a coupled reaction of the type

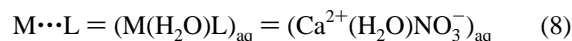


which will be abbreviated as



in the following. In eq 6 (Ca^{2+})_{aq} and (NO_3^-)_{aq} denote the hydrated metal ion (M) and ligand (L), respectively, (Ca^{2+})_{aq} \cdots (NO_3^-)_{aq} is a complex of encounter of the hydrated ions, and ($\text{Ca}^{2+} - \text{NO}_3^-$)_{aq} is an isomer of the complex with different hydration properties. If this still rather unspecific reaction scheme is accepted, the first step of diffusion controlled ion encounter must be so fast that the relaxation process related to it occurs above our frequency range of measurements.

To verify this suggestion let us first apply the Debye–Eigen–Fuoss theory^{30–32} to the idea of Bjerrum ion pair formation.³³ Let us assume the intermediate species in eqs 6 and 7 an outersphere complex:



The stability constant

$$K_1 = \frac{k_{12}}{k_{21}} = \frac{[M(\text{H}_2\text{O})L]}{[M][L]} \quad (9)$$

is then given by the relation

$$K_1 = \frac{4\pi N_A d^3}{3} \exp\left(-\frac{Z_M Z_L e^2}{4\pi\epsilon_0 \epsilon k_B T d}\right) \quad (10)$$

where N_A is Avogadro's constant, d is the distance of approach of the hydrated ions in the outersphere complex, $Z_M (=2)$ and $Z_L (=1)$ are the valencies of the cation and the ligand, respectively, e is the elementary charge, ϵ_0 and k_B denote the electric field constant and Boltzmann's constant, respectively, and $\epsilon (=78)$ is the (relative) permittivity of the solution. Using $d = 0.65$ nm as an upper limit of the distance of ion centers, $K_1 = 5.6$ (mol/L) $^{-1}$ follows. If $d = 0.5$ nm is assumed, $K_1 = 4.9$ (mol/L) $^{-1}$ results for the $\text{Ca}(\text{NO}_3)_2$ system. Though these figures should not be taken without activity corrections to calculate the outersphere complex content of our solutions, they, nevertheless, indicate a high degree of ion complexation. Assuming the diffusional encounter in the coupled reaction (eqs 6 and 7) occurs much faster than the establishment of the equilibrium of structural isomers of the ion complexes, the relaxation rate $1/\tau_1$, associated with the formation of outer sphere complexes from completely dissociated ions, is given by

$$\tau_1^{-1} = k_{12}([M] + [L] + K_1^{-1}) \quad (11)$$

if again activity corrections are neglected. The Debye–Eigen–Fuoss theory^{30–32} predicts

$$k_{12} = \frac{N_A Z_M Z_L e^2}{\epsilon_0 \epsilon k_B T} \frac{D_M + D_L}{\exp\left(\frac{Z_M Z_L e^2}{4\pi\epsilon_0 d k_B T}\right) - 1} \quad (12)$$

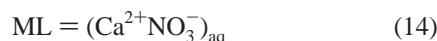
We have calculated the diffusion coefficients D_i , $i = M$ or L , from ionic mobilities λ_i at infinite dilution³⁴ using the Nernst equation

$$D_i = \frac{N_A k_B T}{|Z_i| F^2} \lambda_i, \quad i = M \text{ or } L \quad (13)$$

and found $k_{12} = 3.3 \times 10^{10}$ (mol/L) $^{-1}$ s $^{-1}$ for the ion pair with charge center distance $d = 0.65$ nm. In eq 13, F denotes Faraday's constant. For our $\text{Ca}(\text{NO}_3)_2$ solutions with salt concentration $c \geq 0.2$ mol/L, according to eq 11 $\tau_1^{-1} \geq 2.5 \times 10^{10}$ s $^{-1}$ holds. Hence, the relaxation frequency $(2\pi\tau_1)^{-1}$ associated with the first step in the coupled reaction scheme, is larger than 4 GHz. Consequently, we expect the dissociated ions/outersphere complex equilibrium to contribute to the ultrasonic spectrum above our measuring range.

Ion Pair Structural Isomerization

Since the treatment of the first step in the coupled reaction scheme (eqs 6 and 7) of ion complex formation is in conformity with the idea of an outersphere complex, we assume the second step to reflect an equilibrium between this complex and a more stable contact ion pair



As for both CaCl_2 and $\text{Mg}(\text{NO}_3)_2$ aqueous solutions, the amplitude A of the ultrasonic relaxation associated with the equilibrium, is much smaller than with the calcium nitrate solutions of similar salt concentrations, we suggest the $(\text{Ca}^{2+}\text{NO}_3^-)_{\text{aq}}$ complex is stabilized by favorable interactions of the small calcium ion with sites of high electrically negative charges at the lone pair electrons of the nitrate ion. These interactions may lead to a higher ion pair concentration than the ion complex formation of Ca^{2+} with the symmetrical electron shell of the chloride ion. The smaller Mg^{2+} ion seems to be at

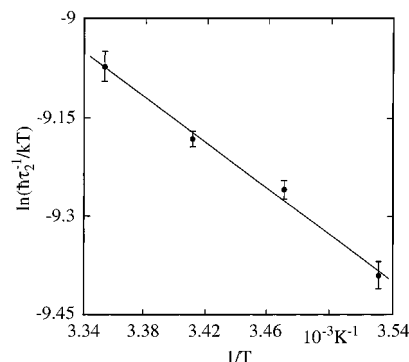


Figure 5. Eyring representation of the relaxation rate τ_2^{-1} for the 1 M aqueous solution of $\text{Ca}(\text{NO}_3)_2$.

a disadvantage here because of stronger interactions with its hydration water. The relaxation frequency values $(2\pi\tau)^{-1}$ derived from our experimental spectra are on the order of 500 MHz (Figures 3 and 4) and are thus substantially smaller than the relaxation frequency estimated for the diffusional ion encounter. We thus start to treat the second step in eqs 6 and 7 as being decoupled from the first one. Hence it is assumed that, on the time scale of the isomerization reaction, the content of the dissociated ions and outersphere complex structures is always in equilibrium.

Assuming a Gibbs free energy of activation,

$$\Delta G_{32}^\# = \Delta H_{32}^\# - T\Delta S_{32}^\# \quad (15)$$

for the reverse reaction, the inverse relaxation time τ^{-1} of ultrasonic excess absorption (eq 2) is identified with the relaxation rate τ^{-1}_2 of the second step of relaxation scheme (eqs 6 and 7), for which^{35,36}

$$\ln\left(\frac{h\tau^{-1}_2}{kT}\right) = \frac{\Delta S_{32}^\#}{R} + \ln(1 + K_2) + \frac{\Delta H_{32}^\#}{RT} \quad (16)$$

follows. Herein

$$K_2 = \frac{k_{23}}{k_{32}} = \frac{[\text{ML}]}{\text{M}(\text{H}_2\text{O})\text{L}} \quad (17)$$

is the equilibrium constant. The slope of relation 16

$$a_2 = d \ln\left(\frac{h\tau^{-1}_2}{kT}\right) / dT^{-1} = -\frac{\Delta H_{32}^\#}{R} - \frac{K_2}{1 + K_2} \frac{\Delta H_2}{R} \quad (18)$$

is independent of temperature (Figure 5). This experimental result indicates that ΔH_2 is small, because otherwise the temperature dependence of the equilibrium constant K_2 would result in a T dependence of a_2 . The equilibrium constant is related to the reaction enthalpy $\Delta H_2 = \Delta H_{23}^\# - \Delta H_{32}^\#$ according to the van't Hoff equation

$$K_2 = \exp(-\Delta H_2/RT) \quad (19)$$

If $\Delta H_2 = 0$ is assumed, $\Delta H_{32}^\# = 14.6$ kJ mol $^{-1}$ and $\Delta S_{32}^\# = -32$ J mol $^{-1}$ K $^{-1}$ are compatible with our experimental relaxation rates (Figure 5). The relaxation amplitude A (eq 2) according to

$$A = \frac{\pi\Gamma c_{\text{soo}}^2 \rho}{RT} \Delta V_{s2}^2 \quad (20)$$

is related to the isentropic volume change

$$\Delta V_{s2} = \frac{\mathcal{A}_\infty}{\rho c_{p\infty}} \Delta H_2 - \Delta V_2 \quad (21)$$

In eqs 19 and 20, $c_{s\infty}$ ($\approx c_s$), \mathcal{A}_∞ , and $c_{p\infty}$ are the high-frequency limiting values of the sound velocity, the thermal expansion coefficient, and the heat capacity at constant pressure, respectively, and ΔV_2 is the isothermal reaction volume. The stoichiometric factor Γ is given by

$$\Gamma^{-1} = [M\cdots L]^{-1} + [ML]^{-1}, \quad (22)$$

thus

$$\Gamma = \frac{K_2}{1 + K_2} [M\cdots L] = \frac{K_2}{1 + K_2} K_1 [M][L] \quad (23)$$

If $K_1 = 1$ is assumed, equivalent with $[M\cdots L] = [ML]$, reasonable isentropic volume changes $\Delta V_{s2} = 9.7$ mL/mol and $\Delta V_2 = 6.6$ mL/mol follow for the 0.2 and 0.5 molar calcium nitrate solutions, respectively. The decrease in the reaction volume with concentration likely reflects the neglect of activity corrections.

Conclusions

Broadband ultrasonic spectra of aqueous solutions of $\text{Ca}(\text{NO}_3)_2$, CaCl_2 , and $\text{Mg}(\text{NO}_3)_2$ reveal a small amplitude relaxation process, indicating ion complex formation in the 2:1 valent electrolyte systems. The relaxation process, with relaxation frequency around 500 MHz reflects a unimolecular reaction, the equilibrium between outersphere and contact-ion complexes. The relaxation amplitude per solute concentration of both latter salt solutions is distinctly smaller than that of the calcium nitrate solutions. Obviously, the interactions of Ca^{2+} ions with nitrate ions are stronger than with chloride ions, probably because the lone electron pairs of the former anion offer sites of comparatively high negative charge density, whereas the Cl^- ion exhibits a symmetrical charge distribution. Therefore, the concentration of calcium chloride contact ion pairs may be smaller. In the $\text{Mg}(\text{NO}_3)_2$ solutions, the ion pair concentration is suggested to be smaller, because hydration water molecules will more strongly interact with the Coulombic field of the smaller cation ($r(\text{Mg}^{2+}) = 0.65 \text{ \AA}$, $r(\text{Ca}^{2+}) = 0.99 \text{ \AA}$).³⁷

Acknowledgment. Financial support by the DAAD (Bonn, Germany) is gratefully acknowledged by one of the authors (P.M.).

References and Notes

- (1) Barthel, J. M. G.; Krienke, H.; Kunz, W. *Physical Chemistry of Electrolyte Solutions*; Steinkopff: Darmstadt, 1998.
- (2) Strehlow, H. *Rapid Reactions in Solution*; VCH: Weinheim, 1992.
- (3) Eggers, F.; Kaatze, U. *Meas. Sci. Technol.* **1996**, *7*, 1.
- (4) Kaatze, U.; Hushcha, T. O.; Eggers, F. *J. Sol. Chem.* **2000**, *29*, 299.
- (5) Tamm, K. In *Encyclopedia of Physics*; Flügge, S., Ed.; Springer: Berlin, 1961; Vol. 11, Part 1.
- (6) Eigen, M. In *Fast Reactions and Primary Processes in Chemical Kinetics, Proceedings of the 5th Nobel Symposium*; Claesson, S., Ed.; Almqvist & Wiksell: Stockholm, 1967.
- (7) Stuehr, J. E. In *Investigation of Rates and Mechanisms of Reactions, Techniques of Chemistry*; Bernasconi, C. F., Ed.; Wiley: New York, 1986; Vol. 6, Part 2.
- (8) Petrucci, S. In *Ionic Interactions*; Petrucci, S., Ed.; Academic: New York, 1971; Vol. 6, Part 2.
- (9) Eigen, M.; Kurtze, G.; Tamm, K. *Z. Elektrochem.* **1953**, *57*, 103.
- (10) Eigen, M.; Tamm, K. *Ber. Bunsen-Ges. Phys. Chem.* **1962**, *66*, 93.
- (11) Eigen, M.; Tamm, K. *Ber. Bunsen-Ges. Phys. Chem.* **1962**, *66*, 107.
- (12) Eigen, M. *Ber. Bunsen-Ges. Phys. Chem.* **1963**, *67*, 753.
- (13) Bonson, A.; Knoche, W.; Berger, W.; Giese, K.; Petrucci, S. *Ber. Bunsen-Ges. Phys. Chem.* **1978**, *82*, 678.
- (14) Kaatze, U.; Wehrmann, B. *Z. Phys. Chem.* **1992**, *177*, 9.
- (15) Saenger, W. *Principles of Nucleic Acid Structure*; Springer: New York, 1994.
- (16) Rongère, Ph.; Morel-Desrosiers, N.; Morel, J.-P. *J. Chem. Soc., Faraday Trans.* **1995**, *91*, 2771.
- (17) Cowman, M.; Eggers, F.; Eyring, E. M.; Horoszewski, D.; Kaatze, U.; Kreitner, R.; Petrucci, S.; Klöppel-Riech, M.; Stenger, J. *J. Phys. Chem. B* **1999**, *103*, 259.
- (18) Kumpf, R. A.; Dougherty, D. A. *Science* **1993**, *261*, 1708.
- (19) Chi, C.; Kim, K. S. *J. Phys. Chem. A* **1999**, *103*, 2751.
- (20) Atkinson, G.; Emar, M. M.; Fernández-Prini, R. *J. Phys. Chem.* **1974**, *78*, 1913.
- (21) Robinson, R. A.; Stokes, R. H. *Electrolyte Solutions*; Butterworths: London, 1959.
- (22) Eigen, M.; Kustin, K. *ICSU Rev.* **1963**, *5*, 97.
- (23) Kaatze, U.; Wehrmann, B.; Pottel, R. *J. Phys. E: Sci. Instrum.* **1987**, *20*, 1025.
- (24) Kaatze, U.; Lautscham, K.; Brai, M. *J. Phys. E: Sci. Instrum.* **1988**, *21*, 98.
- (25) Kaatze, U.; Kühnel, V.; Menzel, K.; Schwerdtfeger, S. *Meas. Sci. Technol.* **1993**, *4*, 1257.
- (26) Kaatze, U.; Kühnel, V.; Weiss, G. *Ultrasonics* **1996**, *34*, 51.
- (27) Lautscham, K.; Wente, F.; Schrader, W.; Kaatze, U. *Meas. Sci. Technol.* **2000**, *11*, 1432.
- (28) Bilaniuk, N.; Wong, G. S. K. *J. Acoust. Soc. Am.* **1993**, *93*, 1609.
- (29) Marquardt, D. W. *J. Soc. Ind. Appl. Math.* **1963**, *2*, 2.
- (30) Fuoss, R. M. *J. Am. Chem. Soc.* **1958**, *80*, 5059.
- (31) Debye, P. *J. Electrochem. Soc.* **1942**, *82*, 265.
- (32) Eigen, M. *Z. Phys. Chem. N. F.* **1954**, *1*, 176.
- (33) Bjerrum, N. K. *Dan. Vidensk. Selsk.* **1926**, *7*, 9.
- (34) Harned, H. S.; Owen, B. B. *The Physical Chemistry of Electrolyte Solutions*; Reinhold Publishing: New York, 1950.
- (35) Eisenberg, D.; Kauzmann, W. *The Structure and Properties of Water*; Clarendon: Oxford, U.K., 1969.
- (36) Rodriguez, L. J.; Eyring, E. M.; Petrucci, S. *J. Phys. Chem.* **1989**, *93*, 6356.
- (37) Conway, B. E. *Ionic Hydration in Chemistry and Biophysics*; Elsevier: Amsterdam, 1981.